



Article scientifique

Article

2023

Published version

Open Access

This is the published version of the publication, made available in accordance with the publisher's policy.

---

## Past human expansions shaped the spatial pattern of Neanderthal ancestry

---

Quilodran, Claudio; Rio, Jérémy Marc Xavier; Tsoupas, Alexandros; Currat, Mathias

### How to cite

QUILODRAN, Claudio et al. Past human expansions shaped the spatial pattern of Neanderthal ancestry. In: Science advances, 2023, vol. 9, n° 42, p. eadg9817. doi: 10.1126/sciadv.adg9817

This publication URL: <https://archive-ouverte.unige.ch/unige:172693>

Publication DOI: [10.1126/sciadv.adg9817](https://doi.org/10.1126/sciadv.adg9817)



## HUMAN GENETICS

# Past human expansions shaped the spatial pattern of Neanderthal ancestry

Claudio S. Quilodrán<sup>1\*†</sup>, Jérémy Rio<sup>1†</sup>, Alexandros Tsoupas<sup>1</sup>, Mathias Currat<sup>1,2\*</sup>

The worldwide expansion of modern humans (*Homo sapiens*) started before the extinction of Neanderthals (*Homo neanderthalensis*). Both species coexisted and interbred, leading to slightly higher introgression in East Asians than in Europeans. This distinct ancestry level has been argued to result from selection, but range expansions of modern humans could provide an alternative explanation. This hypothesis would lead to spatial introgression gradients, increasing with distance from the expansion source. We investigate the presence of Neanderthal introgression gradients after past human expansions by analyzing Eurasian paleogenomes. We show that the out-of-Africa expansion resulted in spatial gradients of Neanderthal ancestry that persisted through time. While keeping the same gradient orientation, the expansion of early Neolithic farmers contributed decisively to reducing the Neanderthal introgression in European populations compared to Asian populations. This is because Neolithic farmers carried less Neanderthal DNA than preceding Paleolithic hunter-gatherers. This study shows that inferences about past human population dynamics can be made from the spatiotemporal variation in archaic introgression.

## INTRODUCTION

Sequencing of Neanderthal genomes has revealed that ~2% of the DNA of modern humans (MHs) outside of Africa is more similar to DNA from Neanderthals (NEs) than it is to DNA from sub-Saharan African populations (1, 2). Two main and nonexclusive hypotheses have been proposed to explain this pattern: (i) hybridization between NEs and MHs during their expansion out of Africa (OOA), leading to the introgression of Neanderthal DNA segments into MHs (1, 2), and (ii) incomplete lineage sorting resulting from ancestral population structure in Africa, with ancestors of non-Africans more closely related to NEs than to sub-Saharan Africans (3). Evidence in favor of hybridization has accumulated during the past decade (4–6). However, the number, timing, and locations of interbreeding events between MH and NE remain unclear. While early studies have suggested a single hybridization pulse in the Middle East (1, 2), a growing body of research supports the hypothesis of multiple hybridization events (7–11). In particular, it has been shown that multiple hybridization events over time and space in western Eurasia are consistent with the levels of Neanderthal ancestry observed in modern populations (7).

While NE ancestry is relatively uniform among modern Eurasian populations (1, 2), it is approximately 8 to 24% higher in East Asia than in Europe (5, 10, 12, 13). This observation is unexpected since the currently known geographic distribution of NEs was almost exclusively in the western part of Eurasia (14). Three major hypotheses have been proposed to explain the difference in NE ancestry between western and eastern Eurasian populations: (i) higher effective population size in Europeans compared to Asians, which led to a stronger effect of purifying selection acting on deleterious NE alleles in the former (15); (ii) dilution of NE ancestry in

Europeans due to an input from a hypothetical “basal” (or “ghost” population) with little or no NE ancestry (16, 17); and (iii) multiple pulses of NE introgression, where the original Eurasian introgression pulse was supplemented by additional pulses after the divergence between the European and Asian populations, resulting in different NE ancestry levels (9, 10, 17, 18).

Recently, an additional hypothesis has been proposed, where different levels of NE ancestry between western Europe and eastern Asia are the result of the range expansion of MHs after the OOA event (19). Population range expansions have important evolutionary consequences, including (i) creating gradients of allele frequencies (20, 21); (ii) increasing the frequency of specific alleles, whether neutral (22, 23) or under natural selection (24, 25); (iii) decreasing genetic diversity along the axis of expansion (26, 27); and (iv) increasing mutational load in populations through the maintenance of deleterious alleles (28). In addition, when admixture with a local population occurs, population expansions tend to disproportionately increase the genetic contribution of the local population to the invasive genetic pool, even if interbreeding is limited (29). This latter effect is expected to result in the formation of spatial gradients of introgression along the axis of the biological invasion (see Fig. 1A). Under this assumption, introgression of local genes (i.e., NEs) increases in the invasive population (i.e., MHs) with the distance from the source of the expansion (i.e., Africa). This is due to the combined effects of (i) continuous hybridization events at the wave front of the range expansion, resulting in more interbreeding possibilities when moving away from the source; (ii) genetic surfing resulting from serial founder effects and population growth; and (iii) demographic imbalance between the growing expanding population and the local population at demographic equilibrium. This hypothesis proposes to explain the different levels of Neanderthal ancestry in Europe and East Asia by different geographical distances from the source of the MH expansion in Africa (19). This assumption of multiple hybridization events occurring continuously across time and space may not be distinguishable from a single hybridization pulse, as defined by Di Santo *et al.* (30). Computational

<sup>1</sup>Department of Genetics and Evolution, University of Geneva, Geneva, Switzerland. <sup>2</sup>Institute of Genetics and Genomics in Geneva (IGE3), University of Geneva, Geneva, Switzerland.

\*Corresponding author. Email: claudio.quilodran@unige.ch (C.S.Q.); mathias.currat@unige.ch (M.C.)

†These authors contributed equally to this work.

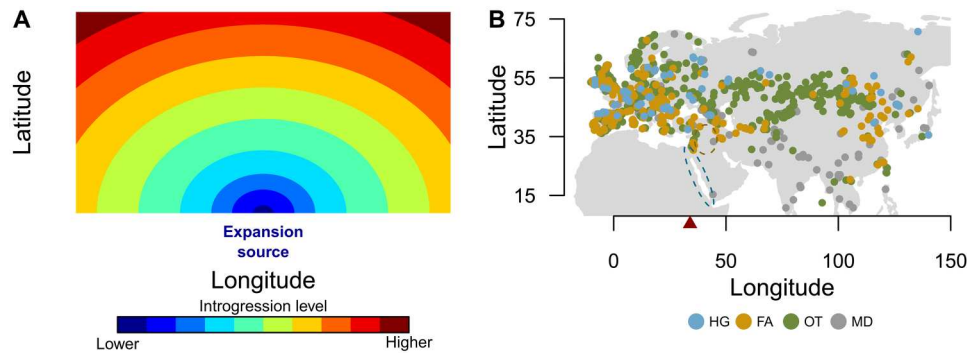


**Fig. 1. Expected ancestry after range expansion and paleogenomic dataset.** (A) Schematic representation of the expected spatial gradient of introgression from the local taxon into an invasive taxon after a biological invasion with hybridization in the case of a uniform environment where both taxa occur everywhere. (B) Distribution of samples in Eurasia used for elucidating spatial gradients of Neanderthal ancestry in MHs. The colored dots represent paleogenomic samples of hunter-gatherers (HGs; ~40,000 to 6000 years BP,  $n = 129$ ), early farmers (FAs; ~10,000 to 2000 years BP,  $n = 679$ ), other ancient (OTs; ~6400 to 300 years BP,  $n = 1726$ ), and modern (MDs; current time,  $n = 91$ ). The dotted ellipse represents the presumed geographic source of the Paleolithic OOA expansion into Eurasia (~50,000 years BP), and the dotted circle represents the source of the Neolithic expansion of agricultural populations from the Fertile Crescent (~11,000 years BP). The red triangle represents the longitudinal limit (34°) that, in our study, separates European ( $n = 1517$ ) from Asian ( $n = 1108$ ) population samples.

simulations showed that the process of range expansion could explain the difference in NE ancestry between Europe and East Asia based on contemporary genomic information from the two extreme sides of Eurasia (west and east) (19). However, neither a detailed inspection of geographic introgression patterns (i.e., the existence of gradients) nor their change over time was included in this study. In addition, range expansions occurred not only during the OOA expansion (7) but also during other prehistoric periods (31). This includes the European Neolithic transition, when farmers coming from southeast Europe and Anatolia partially replaced hunter-gatherers (32–35), as well as the Bronze Age, with the spread of pastoralist populations from Eurasian steppes (36–38). Therefore, multiple population movements during recent human history could have contributed to shaping NE ancestry across time and space because distinct expanding populations can carry various levels of NE ancestry (20, 31, 39).

Here, we investigate whether spatial gradients of introgression consistent with the range expansion hypothesis have occurred in Eurasia by examining the levels of NE ancestry in human populations distributed across space and time. Our study demonstrates

that spatiotemporal levels of introgression provide valuable information about past population dynamics, suggesting multiple episodes of range expansion as a major driver for shaping archaic introgression levels during human evolutionary history.

## RESULTS AND DISCUSSION

### Spatial gradients of Neanderthal ancestry in Eurasia

We analyzed an extended dataset of 4464 published ancient and modern genomes [from ~40,000 years before the present (BP) to present time] retrieved from the Allen Ancient DNA database (40). We associated each genome with one of the following population groups: Paleolithic/Mesolithic hunter-gatherers (HGs), Neolithic/Chalcolithic farmers (FAs), other ancient samples (OTs), or modern samples (MDs). We estimated NE introgression using  $F_4$  ratios for all genomes and averaged the values for genomes from the same geographic coordinates, time periods, and population group, leading to  $n = 2625$  samples constituted of one or more genomes (Fig. 1B; see Material and Methods). We then explored the fixed effect of latitude, longitude, time (dates in years BP), continental area (Europe or Asia), and their interactions by using a linear mixed model (LMM) with log-transformed NE ancestry as the response variable. LMMs are particularly useful for dealing with hierarchical structures and the nonindependence of the dataset. We investigated the random effect of the population group, the period nested within these groups (in clusters of 500 years), and the spatial and temporal autocorrelation of data. This model was called "Full Eurasia" because it uses the whole dataset. On the basis of the lowest Akaike information criterion (AIC) value (41), the best LMM was retained (table S1).

By considering the average date of all samples as a time reference (~4200 years BP), we observed a linear relationship of NE ancestry with latitude and longitude, in both Europe and Asia (Fig. 2 and table S1). These geographic patterns support the hypothesis of spatial introgression gradients generated after population expansion with hybridization [(19), simulations in text S1 and data S1], schematically represented in Fig. 1A, in which the introgression of local genes (i.e., NEs) is expected to increase in the invasive population

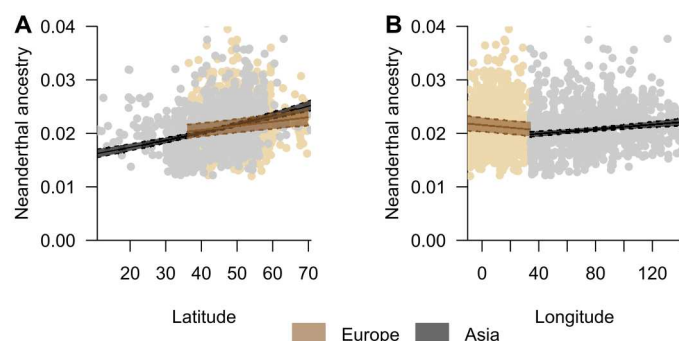


**Fig. 2. Effects of latitude and longitude on the level of Neanderthal ancestry in both Europe and Asia.** (A) Effect of latitude and (B) effect of longitude. The solid and dotted lines represent the estimated values and 95% confidence intervals, respectively. The colored dots represent the distribution of the full dataset of ancient and modern DNA samples used in the Full Eurasia analysis ( $n = 2625$ ).

(i.e., MHs) with the distance from the source of its expansion (i.e., Africa). While a positive relationship with latitude is observed in Europe and Asia (Fig. 2A), a contrasting relationship is observed with longitude, positive in Asia and negative in Europe (Fig. 2B). The increasing NE introgression with latitude is compatible with the OOA expansion of MHs from southern to northern areas of Eurasia while hybridizing with NEs. The longitudinal pattern is compatible with a source of expansion in the Middle East, from which NE ancestry is expected to increase with longitude in Asia but decrease with longitude in Europe. Although alternative evolutionary forces may also be responsible for creating introgression gradients (e.g., spatially varying selective pressure), the specific pattern we observed with a source of all spatial gradients in the Middle East makes population range expansion the most parsimonious explanation.

Alternatively, spatial variation of NE ancestry in MH could result from an unequal distribution of NEs in Eurasia, with more interspecific interactions occurring in areas where NEs were more numerous, resulting in distinct patterns of local hybridization. We find a higher NE ancestry level in Europe than in Asia after the OOA (Fig. 3), which is in accordance with the current fossil record of NEs in Eurasia, with more accumulated evidence in Europe. Moreover, our results showing more NE ancestry in northern Eurasia than in southern Eurasia further concur with evidence of NE presence in the northern Himalayas (14), even if an undetected presence in the south cannot be ruled out. Nevertheless, even in the case of unequal distribution of the local species, increasing gradients of introgression in the invasive population (i.e., MHs) resulting from range expansion may remain a valid explanation. For instance, this is expected after a simulated range expansion where the local population is only occupying a part of the area (text S1) (19), as it may have been the case for NEs in Eurasia.

Similar gradients of spatial introgression are observed when replacing latitude and longitude by the topographic distance from a putative source of the OOA expansion in East Africa (text S2), as well as when computing the  $F_4$  ratio from a dataset presumably less affected by background selection (text S3). However, our analysis does not support the hypothesis that a slightly higher level of NE ancestry in East Asia than in western Europe today could be

explained by the greater distance to the source of the MH expansion in Asia than in Europe (19). This hypothesis was made from modern DNA data only, while our results also considered ancient DNA samples. Using paleogenomic data, we show the reverse pattern for samples older than 20,000 years BP, with more NE ancestry observed in Europe than in Asia (Fig. 3). The current pattern of NE ancestry being higher in Asia than in Europe must thus have developed at a later stage.

### Temporal variation in Neanderthal ancestry

Our results suggest that the longitudinal gradient slope has remained similar over the past 40,000 years (table S1), whereas the latitudinal gradient of NE ancestry has significantly changed over time ( $F = 4.4$ ,  $P = 0.03$ ). The latitudinal pattern is more prominent during the early period in Europe and becomes less visible ~30,000 years BP, together with an overall reduction in NE ancestry (Fig. 3). While this implies that the level of NE ancestry in Eurasia may not have been uniformly distributed across space as is observed today, this expectation needs to be confirmed with more paleogenomes because the interaction between latitude and time is no longer significant when considering the average of all candidate models (based on a cumulative weighted AIC of 90%,  $Sw_i^3$  0.90; table S2) instead of the best model only.

The variation in NE ancestry across time is now debated. It has been proposed that ancient European genomes showed more NE ancestry compared to present-day Europeans (4), but this result was questioned because of a methodological bias in the ancestry estimation procedure (42). Nevertheless, it has been estimated that NE ancestry could have been as high as 10% at the time of admixture before decreasing rapidly to the current rate of ~2% (43). Here, we show that the temporal reduction in NE ancestry is linked to latitude. The southern samples in Europe show an almost constant NE ancestry through time, while the northern samples experienced a reduction between approximately 40,000 and 20,000 years BP. The latitudinal gradient could have undergone important changes, possibly due to population expansions and contractions experienced by MHs during the Last Glacial Maximum (LGM) or other more limited ice ages. Our results show that this gradient becomes less evident in modern data (Fig. 3). Because the longitudinal pattern

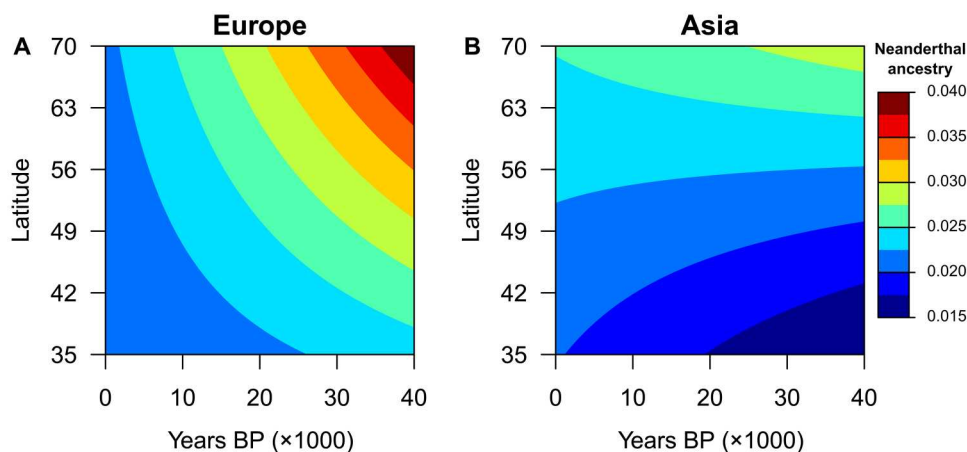


**Fig. 3. Influence of latitude and time on the level of Neanderthal ancestry.** (A) Ancestry level in Europe and (B) ancestry level in Asia. The analysis considers the full dataset of ancient and modern DNA samples (Full Eurasia,  $n = 2625$ ). The y axis corresponds to the range where both regions (Asia and Europe) have the most data.



has been less affected during the past 40,000 years, it may represent a relict signature of the OOA range expansion that occurred during MH evolution between ~60,000 and 45,000 years BP.

Natural selection has been invoked to explain the reduction in NE ancestry over time (15, 44), but different historical processes could have also played an important role. This includes population expansions and contractions (45, 46), as well as interactions between genetically differentiated populations with different levels of NE ancestry (16, 17). In Europe, a prominent genetic transition occurred during the spread of early Neolithic farmers, when they partially replaced Paleolithic/Mesolithic hunter-gatherers [i.e., the so-called Neolithic transition (33, 34, 35)]. At least along the Danube route from Anatolia to Central Europe, paleogenetic analyses have revealed that the first stage of the Neolithic transition occurred through the migration of FAs, followed by admixture with local HGs in a second stage, e.g., (32, 33, 35, 47). This transition began in the Fertile Crescent ~11,000 years BP (48), and its consequences on the distribution of NE ancestry have been weakly explored thus far (16).

### Less Neanderthal ancestry in early farmers than hunter-gatherers in Europe

We thus explored more specifically the variation in the level of NE ancestry across time and population groups (HGs, FAs, and OTs,  $n = 2534$  in total). The OT group includes all ancient samples that are neither FAs nor HGs, including, for example, the Bronze Age and more recent periods. Samples from the MD group were excluded from this analysis because they do not allow us to explore temporal variation in NE ancestry (all modern data are associated with the same date). We included population groups, continental area (either Europe or Asia), time, and their interactions as fixed variables, also correcting for spatial autocorrelation in the dataset. This model is called "Ancient Eurasia" because it only considers ancient samples, and its best LMM is presented in table S1. We observed an influence of time on the differences between Europe and Asia ( $F = 9.22$ ,  $P < 0.01$ ) and population groups ( $F = 9.41$ ,  $P < 0.01$ ), with an overall higher NE ancestry level for HGs than for FAs, particularly visible in Europe (Fig. 4). At approximately 10,000 years BP, when the first FA appeared in the Near East, the difference

between FAs and HGs was significant in Europe [HG:  $0.024 \pm 0.001$  (estimated mean  $\pm$  SE), FA:  $0.019 \pm 0.001$ ,  $t$  ratio =  $-6.14$ ,  $P < 0.001$ ], as well as in Asia (HG:  $0.022 \pm 0.001$ , FA:  $0.018 \pm 0.001$ ,  $t$  ratio =  $-6.14$ ,  $P < 0.001$ ). Approximately 6000 years BP, when farming was well established but some HG populations persisted, the difference in NE ancestry was still significant between the HG ( $0.023 \pm 0.001$ ) and FA ( $0.020 \pm 0.0002$ ) populations in Europe ( $t$  ratio =  $-4.21$ ,  $P < 0.001$ ), as well as between the HG and OT ( $0.020 \pm 0.0003$ ) populations ( $t$  ratio =  $3.51$ ,  $P = 0.001$ ), but not between the FA and OT populations ( $t$  ratio =  $-0.41$ ,  $P = 0.91$ ). A similar situation was observed in Asia at this time (FAs versus HGs,  $t$  ratio =  $-4.26$ ,  $P < 0.001$ ; HGs versus OTs,  $t$  ratio =  $3.51$ ,  $P = 0.001$ ; FAs versus OTs,  $t$  ratio =  $-0.41$ ,  $P = 0.91$ ). Overall, this means that earlier FAs carried less NE ancestry than the former HGs of the same area. This difference vanished over time, since the level of NE ancestry in FAs increased during the cohabitation period with HGs in both geographic regions (Fig. 4). Admixture between late HGs and FAs could possibly explain part of the decrease in NE ancestry in HG over time, but it is probably not the only factor since this decrease appears to have started before the appearance of farming ~10,000 years BP (Fig. 4). However, this result should be interpreted with caution since the ancient samples are scarce and even absent between 30,000 and 20,000 years BP. Further data and studies could help shed light on this specific point. While Asian FAs reached an average level similar to that of HGs, European FAs did not reach such a high level (Fig. 4). Thus, FAs could have acted as a population that diluted NE ancestry in western Eurasia (text S4), as previously suggested (16, 17).

Multiple episodes of range expansion of populations where levels of NE ancestry differed could provide an explanation for the spatio-temporal change in NE ancestry. Our results support our former hypothesis that past human range expansions (i.e., HGs then FAs) contributed to the creation of spatial gradients of NE ancestry, with the level increasing from their source in southwest Asia (Figs. 2 and 3). During the OOA, HGs accumulated NE introgression as they expanded, in accordance with the range expansion hypothesis (19). The second range expansion into western Eurasia, that of early FAs, is critical to explain the overall dilution of NE ancestry in this area. The earliest FAs derived from HG populations in Anatolia and the Levant, with a lower level of NE ancestry than HG populations in the rest of Europe, as expected from their geographic proximity to the source of the OOA expansion (see text S4). The later expansion of the steppe pastoralists does not seem to have had as much influence as there is not a significant difference between the FA and OT population groups, but this would require a more detailed examination, as our OT group includes populations from different cultural periods.

### Spatial gradients in European farmers and hunter-gatherers

We then decided to focus our analysis on Europe due to the larger density and more uniform distribution of paleogenomes than in Asia, where the Paleolithic and Neolithic eras are represented by a lower number of samples that cover a larger area (1517 samples in Europe versus 1108 samples in Asia for an area four times as large; Fig. 1B). Moreover, domesticated plants and animals occurred in more than one site in Asia (49, 50), making exploration of past FA population dynamics more challenging than in Europe.

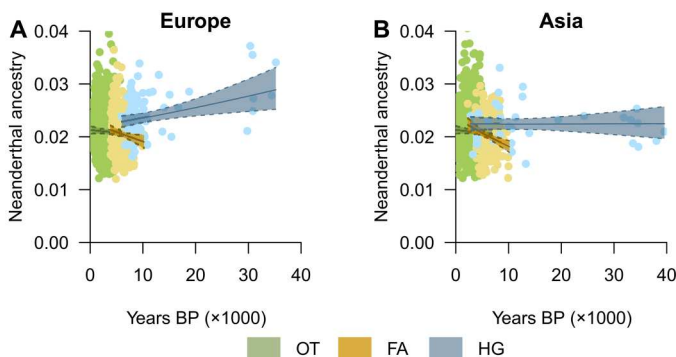


**Fig. 4. Temporal variation in the level of Neanderthal ancestry in different cultural populations.** HG, hunter-gatherers; FA, Neolithic farmers; OT, other ancient samples. (A) Ancestry level in Europe and (B) ancestry level in Asia. The solid and dotted lines represent the estimated values and 95% confidence intervals, respectively. The colored dots represent the distribution of ancient DNA samples used in the best Ancient Eurasia analysis ( $n = 2534$ ).

By using a subsample of data restricted to Europe ( $n = 1517$ ), we explored the effect of latitude, longitude, and population groups (HG-FA-OT-MD) on NE ancestry, controlling for the fixed effect of time. We excluded cross-level interactions between time and population groups because of the lack of temporal variation in MD samples. The LMM is called "Europe," and its best version is presented in table S1. The interaction between longitude and population group was nonsignificant and excluded during model selection, together with the interaction between latitude and population groups (tables S1 and S2). While we cannot exclude that the absence of differences between populations could result from a lack of power, this implies that the negative longitudinal and positive latitudinal trends shown in Fig. 2 remain for all population groups in Europe, despite the higher NE ancestry in HGs compared to other cultural populations (Fig. 5). The interaction between latitude and longitude was significant ( $F = 29.29$ ,  $P < 0.001$ ), meaning that their introgression slopes were interdependent for all population groups (Fig. 5 and fig. S1). When considering the full model that includes all fixed variable interactions, the only spatial gradient that has changed is the slope of latitude for HGs compared to FAs ( $F = 2.68$ ,  $P = 0.04$ ; table S3). Although the result for HGs may be influenced by the scarcity of samples during the Paleolithic, this analysis suggests that the latitudinal variation could have changed more than the longitudinal variation during this period (Figs. 3 and 5). Different events of population contractions and expansions during the Paleolithic related to the LGM (45, 46) could have affected the latitudinal gradient more than the one seen for longitude. Overall, the spatial trend remains similar across different periods of time, becoming less pronounced in MD samples (fig. S1) and with a higher NE ancestry in HGs (Fig. 5).

In Europe, both the early human expansion during the Paleolithic and the farming expansion during the Neolithic trace back to southwest Asia (31), where we estimated the lowest level of NE ancestry. The difference in NE ancestry between HGs in Europe and in

Anatolia, where FAs originated (see red area and blue area for HGs, respectively; Fig. 5), explains why early FAs contributed to an overall reduction in the level of NE ancestry when expanding across Europe (Fig. 5). Note that it was recently found that modern Levantine and southern Arabian populations still have lower NE ancestry than northern Eurasian populations (51).

According to the expansion hypothesis (19), as HGs spread over Europe, their NE introgression levels increased because of a combination of stochastic demographic and migratory processes related to gene dilution (20, 31, 39) and gene surfing (22, 23), which explain the spatial gradients of NE ancestry observed in HGs (Fig. 5). Later, a second expansion occurred during the Neolithic, following approximately the same direction as the expansion of HGs. Consequently, the spatial gradient already present in HGs was maintained in FAs because both populations admixed (Fig. 5). In addition, when analyzing paleogenomes from 10,200 to 3800 years BP, we showed that the FA ancestry is negatively related to NE ancestry in Europe ( $F = 686$ ,  $P < 0.001$ ; text S4). This negative relationship strengthened with the time elapsed since the start of the FA expansion (text S4). As previously noted (45, 46), the sole observation of a south east to north west genetic cline in Europe is not informative about the expansion of FAs, as the cline could have been generated during the previous HG expansion. Here, our results suggest that the NE ancestry cline was produced during the HG range expansion and was affected by the later expansion of FAs during the Neolithic transition while maintaining the same general orientation. As FAs had initially less NE ancestry than HGs, it lowered the average amount in the admixed European population. This corresponds to the model of population expansion with partial replacement supported by paleogenomic studies for the Neolithic (32–34).

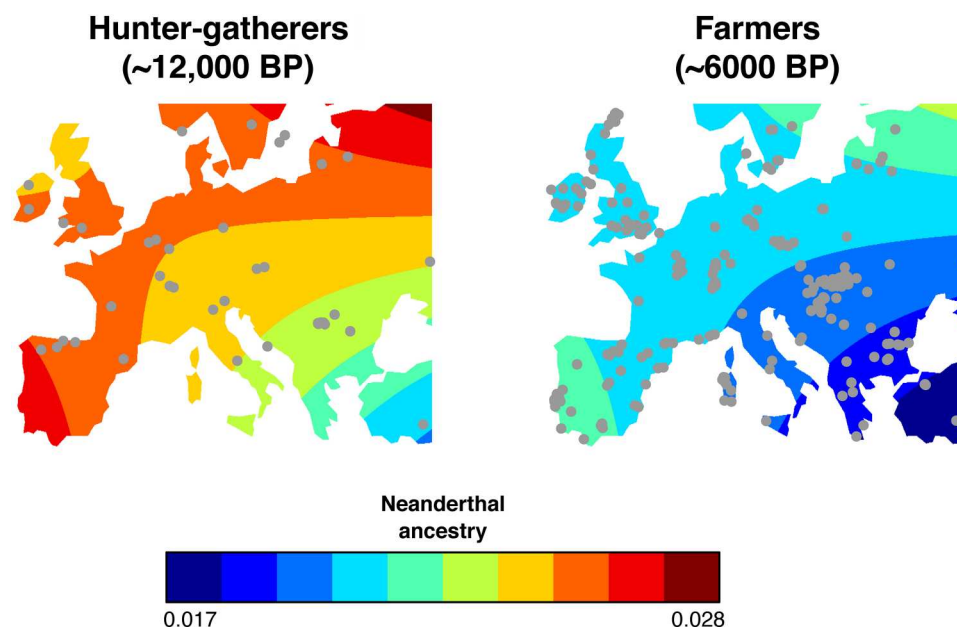


**Fig. 5. Spatial variation on the level of Neanderthal ancestry.** The ancestry levels in European hunter-gatherers and farmers were projected using the best Europe model ( $n = 1517$ ). The gray dots represent the distribution of DNA samples.

## Influence of human range expansions on the distribution of Neanderthal ancestry

Our findings highlight the evolutionary impact of past range expansions in generating spatial gradients of NE ancestry in MHs. We observed that these ancestry levels were more spatially heterogeneous in the past and that they became more homogeneous during the Holocene under the effect of gene flow resulting from population movements and migrations. Complex population movements and genetic interactions are reflected when analyzing the level of NE ancestry in different regions (Europe and Asia) and in populations with different cultural backgrounds (HGs and FAs). The spatial gradient of NE ancestry in HGs is compatible with a model of range expansion of MHs during the OOA expansion. After this first expansion, the level of NE ancestry was slightly higher in western Eurasia than in eastern Eurasia. Then, a second range expansion of early FAs with a lower NE ancestry than HGs occurred in Europe during the Neolithic transition, from the southeast toward the northwest. This second range expansion is essential for explaining the pattern currently observed of lower NE ancestry in western Europe than in East Asia (5, 10, 12, 13). Our results therefore do not support the hypothesis that the slightly greater NE ancestry in eastern Eurasia compared to western Eurasia is due to population dynamics during the OOA expansion of MHs taking place ~40,000 years BP. Instead, our results reveal that the current geographical heterogeneity of NE ancestry is due to dynamics that occurred during the more recent Neolithic expansion ~10,000 years BP. The early FA populations admixed with HG, leading to a progressive increase in HG ancestry and, consequently, NE ancestry in the expanding FA populations. It has been proposed that the early FAs are partly genetically derived from the previously identified "basal Eurasian" lineage (16, 17, 51). This lineage is thought to have diverged from other Eurasian HG populations before the latter mixed with the NE, and therefore had a lower NE ancestry (16, 17, 51). It has been suggested that its original location could have been the Arabian Peninsula (52), which is close to the source of the OOA expansion and therefore compatible with the range expansion hypothesis. The partial replacement of HGs by FAs (32, 33) thus contributed to reducing the level of NE ancestry in western Eurasia more than in eastern Eurasia. While selection was invoked to explain the difference between Europe and Asia (44), the neutral hypothesis of historical range expansions is sufficient to explain past and current patterns of NE ancestry in humans. This model does not exclude the possibility that differences in population sizes (15) or in generation time (53) between eastern and western Asia may also have played a role in shaping NE ancestry patterns, but a modeling study focusing on these aspects would be necessary as the effect of population dynamics and life history traits on genetic diversity in a spatial context is not trivial to assess. Furthermore, the relationship between the range expansion model and the number of admixture pulses depends on the definition of a pulse. Our results are consistent with a continuous series of hybridization events distributed in time and space during the OOA expansion, which could be considered as one major admixture pulse (30). Although the introgression of archaic material in MHs was probably counterselected during an initial stage (42), the fact that the amount of NE introgression is relatively stable through time, approximately 2%, suggests that this remaining small portion of introgressed DNA can be considered to evolve generally neutrally or near-neutrally. This assumption is also supported by the

observation that archaic introgression tends to be rarer in gene-rich regions (15). However, there are exceptions to this general pattern, with examples of adaptive introgression related to the immune system (54, 55), skin pigmentation (9), and altitude (56), providing a better adaptation to local environmental conditions and pathogens (57). Moreover, in present-day populations, some loci introgressed from archaic hominins appear to influence disease risk, such as neurological, psychiatric, immunological, dermatological, and dietary disorders (5, 58), either positively or negatively. It is thus crucial to describe neutral patterns of introgression resulting from human demography and migration to allow better detection of loci under selection (positive or negative) as outliers of the neutral background. It could help to reconstruct the impact of past epidemics on the evolution of human immunity. Additional paleogenomic data for the most ancient periods combined with alternative modeling methods should allow a more detailed understanding of evolutionary processes leading to similar diversity patterns. These developments would provide a better understanding of both the population dynamics within our species and its interactions with other extinct archaic species, such as NEs and Denisovans.

## MATERIALS AND METHODS

### Dataset

Paleogenomic data available for Eurasian populations were retrieved from the AADR database [Allen Ancient DNA Resource v50.0 (40)]. This database includes 10,391 genomes. For each genome, we retained the mean date in years BP reported in the database, which corresponds either to the mean of the 95% confidence interval calibrated radiocarbon age or to the mean of the archaeological context range. We only included genomes from individuals located in Eurasia in our analysis, with longitude 34° as a delimiter, i.e., west of 34° is considered Europe in our analyses, while east of 34° is considered Asia. For genomes that have multiple versions in the database, we retained for analysis only the version with the most single-nucleotide polymorphisms. We filtered out putatively contaminated paleogenomes by using the contamination warning estimated through linkage disequilibrium (59) (values of "contamLD\_warning" being either "Model\_Misspecified" or "Very\_High\_Contamination" were removed) as well as by excluding genomes that contained "contam" or "possible.contam" in their GroupID name. Moreover, we excluded from the downstream analysis all the genomes missing the geographical coordinates of their origin or information about the population group to which they belong.

We assigned each genome to a population group based either on the information provided by the GroupID parameter or on the information provided in the publications that produced these genomes: Paleolithic and Mesolithic hunter-gatherers (HGs;  $n = 135$ ), Neolithic and Chalcolithic farmers (FAs;  $n = 810$ ), other ancient genomes not belonging to HG and FA (OTs,  $n = 2327$ ), and modern genomes (MDs;  $n = 1192$ ), which are referenced by a date zero in the database. Data S2 lists all the genomes used in our analysis.

### Estimation of Neanderthal ancestry

We used  $F_4$  ratios as introduced by Reich *et al.* (60) to estimate NE ancestry ( $\alpha$ ) in each genome of interest. It is calculated as the ratio of



two  $F_4$  statistics generated from five populations, where one population results from the admixture between two others. We followed Petr *et al.* (42) to avoid a bias in the temporal distribution of the  $F_4$  statistics. This procedure considers the reflux of NE introgression from European populations into northern and western African populations using the Dinka population from eastern Africa as a sister population ("C") of the tested genome ("X") instead of the Yoruba from western Africa. The Altai Neanderthal ("A") was used as a sister population of the Vindija Neanderthal ("B"), and chimpanzee was included as an outgroup ("O"). The value of  $\alpha$  estimates the proportion of ancestry deriving from B in an admixed genome X, using the same A, C, and O populations as references:  $\alpha = F_4(A, O, X, C)/F_4(A, O, B, C)$ , where X = test genome; A = Altai\_Neanderthal.DG; B = Vindija\_Neanderthal.DG; C = Dinka.DG; O = Chimp.REF, all retrieved from the AADR database. We refer to this observed  $F_4$  ratio as Neanderthal ancestry (or introgression).

We used the R package ADMIXTOOLS 2 to compute the  $F_4$  ratio for each genome (61). Only genomes showing a significant value ( $Z > 3$ ) were included in our analyses to ensure the accuracy of the estimated NE ancestry. This resulted in 4464 genomes. The European area is represented by 2146 paleogenomes, and the Asian area is represented by 2318 paleogenomes. We averaged the  $F_4$  ratio for genomes with the same date, geographic coordinates, and population group, resulting in a final dataset of 2625 population "samples" grouping one or more genomes (from ~40,000 years BP to modern time, 1517 in Europe and 1108 in Asia; Fig. 1B).

### Statistical analysis

We used the computed  $F_4$  ratio as the response variable in a series of LMM analyses, which are especially well suited to describe the relation between variables, including autocorrelation and missing data. We checked the model assumptions of normality and homoscedasticity. The response variable was thus log-transformed to maintain the Gaussian distribution of residuals. In the first analysis, we included latitude, longitude, time (years BP), continental area (Europe or Asia), and their interactions as explanatory (fixed) variables. We evaluated the effect of the population groups (HG, FA, OT, and MD), as well as the nested effect of time period within these population groups (i.e., grouping dates within 500-year ranges), as random variables. We also evaluated the influence of the spatial autocorrelation and temporal autocorrelation of the dataset. The choice of fixed and random model structures from among those investigated and the selection of the best model was based on the lowest AIC value (41), following Zuur *et al.* (62). The final model structure was an LMM that considered the period nested in the population groups as a random intercept and slope of continental area, as well as an exponential spatial autocorrelation. We called this model Full Eurasia because it incorporates the whole dataset (table S1). Two similar models are presented in the Supplementary Materials. The first included the topographic distance from East Africa (considered as a putative origin of the OOA expansion), which was used as an explanatory variable instead of latitude and longitude (text S2). The second considered the same Full Eurasia model, but using a subset of data restricted to genomic regions with high recombination rates ( $>1.5$  cM/Mb), also removing regions closer than 100 base pairs from conserved elements, following (63). This dataset is much more limited in size ( $n = 1190$ ) and genomic positions (~80% less), but presumably less affected by

background selection, while still affected by GC-biased gene conversion (63). We used this "more neutral" subset to compute the  $F_4$  ratios (text S3).

Because the ancient DNA samples belonging to different population groups were not equally distributed throughout Europe and Asia, we ran two additional LMM analyses using subsets of the data to explore in more detail the fixed effect of population groups on the log-transformed  $F_4$  ratio. The autocorrelation structure, as well as the random and fixed effects of both models, was selected in a similar way as the Full Eurasia model. First, we focused on the temporal trend in Europe and Asia, considering time, continental area, and population groups (HG-FA-OT) as fixed variables, also including their respective interactions in the model. We excluded MD samples because there is no variation allowing a cross-level interaction with time (all dates are identical). The final model structure considered the period (i.e., in clusters of 500 years) as a random intercept and slope of continental area, as well as an exponential spatial autocorrelation. This model is reported as Ancient Eurasia because it considers only the ancient genomes from Eurasia as a whole (table S1). Second, because the spatial density of available paleogenomes (i.e., the number of paleogenomes per million of square kilometers) is much larger in Europe (191.55) than in Asia (28.15), we focused the spatial analysis of population groups on Europe. The fixed variables were latitude, longitude, population groups (HG-FA-OT-MD), and their interactions, also including time as a fixed covariate. The interaction between time and population groups was excluded because of the lack of temporal variation in MD samples. The final LMM considered the period as a random intercept, as well as a ratio quadratic spatial autocorrelation. This model is reported as Europe (table S1). We finally conducted an additional analysis to assess the impact of FA ancestry on the level of NE ancestry of European paleogenomes, which is presented in the Supplementary Materials (text S4).

For all LMM analyses, we verified collinearity among fixed variables by computing the variance inflator factor (VIF). All variables included in the separate models did not show collinearity with other variables ( $VIFs < 4$ ) (62). We reported the conditional  $[R^2_{GLMM(c)}]$  and marginal  $[R^2_{GLMM(m)}]$  coefficients of determination for the selected LMMs (table S4). They denote the proportion of variance explained by fixed variables and both fixed and random variables, respectively (64). Because the number of samples within continental locations and groups of populations were not the same, we reported mean differences by considering an analysis of covariance (ANCOVA) with sum of squares of type III. A Tukey correction was implemented for multiple post hoc comparisons among population groups. We reported trends of continuous variables by considering the average values of other predictors within continental areas and population groups (table S5), except when it is specifically mentioned in the main text. We show the outputs of the best models after the selection of the random and fixed structure (table S1), but we also show the average of candidate models based on a cumulative weighted AIC of 90% ( $Sw_i^3$  0.90; table S2), as well as the full model without selection of fixed variables (table S3). The last two models were referred to when a nonsignificant relationship was excluded from the best models. All analyses were carried out using the R language (65). The nlme package (66) was used for the LMMs, the emmeans package (67) was used for multiple comparisons, and the MuMIn package (68) was used for the estimation of pseudodetermination coefficients and model averaging. The function



predict.lme was used to extrapolate values of NE ancestry with the LMMs. The function filled.contour was used for plotting contour plots, and the raster package (69) was used for plotting the extrapolated values on a map.

## Computational simulations

We performed a series of spatially explicit simulations in the context of species range expansion and hybridization by using the software SPLATCHE3 (70). We evaluated the power of LMMs to detect spatial introgression gradients when the dataset is heterogeneously distributed in space and time, as is the case with the AADR database. We evaluated four scenarios: (i) hybridization during range expansion, heterogeneous dataset; (ii) hybridization during range expansion, homogeneous dataset; (iii) hybridization without range expansion, homogeneous dataset; and (iv) hybridization without range expansion, heterogeneous dataset. Details about the methods and results are presented in the Supplementary Materials (text S1 and data S1).

## Supplementary Materials

**This PDF file includes:**

Tables S1 to S10

Figs. S1 to S6

Texts S1 to S4

Legends for data S1 and S2

**Other Supplementary Material for this manuscript includes the following:**

Data S1 and S2

## REFERENCES AND NOTES

1. R. E. Green, J. Krause, A. W. Briggs, T. Maricic, U. Stenzel, M. Kircher, N. Patterson, H. Li, W. Zhai, M. H. Y. Fritz, N. F. Hansen, E. Y. Durand, A. S. Malaspina, J. D. Jensen, T. Marques-Bonet, C. Alkan, K. Prüfer, M. Meyer, H. A. Burbano, J. M. Good, R. Schultz, A. Aximu-Petri, A. Butthof, B. Höber, B. Höffner, M. Siegemund, A. Weihmann, C. Nusbaum, E. S. Lander, C. Russ, N. Novod, J. Affourtit, M. Egholm, C. Verna, P. Rudan, D. Brajkovic, Ž. Kucan, I. Gušić, V. B. Doronichev, L. V. Golovanova, C. Lalueza-Fox, M. de la Rasilla, J. Fortea, A. Rosas, R. W. Schmitz, P. L. F. Johnson, E. E. Eichler, D. Falush, E. Birney, J. C. Mullikin, M. Slatkin, R. Nielsen, J. Kelso, M. Lachmann, D. Reich, S. Pääbo, A draft sequence of the Neandertal genome. *Science* **328**, 710–722 (2010).
2. D. Reich, R. E. Green, M. Kircher, J. Krause, N. Patterson, E. Y. Durand, B. Viola, A. W. Briggs, U. Stenzel, P. L. F. Johnson, T. Maricic, J. M. Good, T. Marques-Bonet, C. Alkan, Q. Fu, S. Mallick, H. Li, M. Meyer, E. E. Eichler, M. Stoneking, M. Richards, S. Talamo, M. V. Shunkov, A. P. Derevianko, J. J. Hublin, J. Kelso, M. Slatkin, S. Pääbo, Genetic history of an archaic hominin group from Denisova Cave in Siberia. *Nature* **468**, 1053–1060 (2010).
3. A. Eriksson, A. Manica, Effect of ancient population structure on the degree of polymorphism shared between modern human populations and ancient hominins. *Proc. Natl. Acad. Sci. U.S.A.* **109**, 13956–13960 (2012).
4. Q. M. Fu, The genetic history of Ice Age Europe. *Nature* **534**, 200 (2016).
5. K. Prüfer, A high-coverage Neandertal genome from Vindija Cave in Croatia. *Science* **358**, 655–658 (2017).
6. F. Racimo, S. Sankararaman, R. Nielsen, E. Huerta-Sanchez, Evidence for archaic adaptive introgression in humans. *Nat. Rev. Genet.* **16**, 359–371 (2015).
7. M. Currat, L. Excoffier, Strong reproductive isolation between humans and Neanderthals inferred from observed patterns of introgression. *Proc. Natl. Acad. Sci. U.S.A.* **108**, 15129–15134 (2011).
8. M. Kuhlwlilm, I. Gronau, M. J. Hubisz, C. de Filippo, J. Prado-Martinez, M. Kircher, Q. Fu, H. A. Burbano, C. Lalueza-Fox, M. de la Rasilla, A. Rosas, P. Rudan, D. Brajkovic, Ž. Kucan, I. Gušić, T. Marques-Bonet, A. M. Andrés, B. Viola, S. Pääbo, M. Meyer, A. Siepel, S. Castellano, Ancient gene flow from early modern humans into Eastern Neanderthals. *Nature* **530**, 429 (2016).
9. B. Vernot, J. M. Akey, Resurrecting surviving Neandertal lineages from modern human genomes. *Science* **343**, 1017–1021 (2014).
10. J. D. Wall, M. A. Yang, F. Jay, S. K. Kim, E. Y. Durand, L. S. Stevison, C. Gignoux, A. Woerner, M. F. Hammer, M. Slatkin, Higher levels of Neanderthal ancestry in East Asians than in Europeans. *Genetics* **194**, 199 (2013).
11. K. Prüfer, The complete genome sequence of a Neanderthal from the Altai Mountains. *Nature* **505**, 43–49 (2014).
12. M. Meyer, M. Kircher, M. T. Gansauge, H. Li, F. Racimo, S. Mallick, J. G. Schraiber, F. Jay, K. Prüfer, C. de Filippo, P. H. Sudmant, C. Alkan, Q. Fu, R. do, N. Rohland, A. Tandon, M. Siebauer, R. E. Green, K. Bryc, A. W. Briggs, U. Stenzel, J. Dabney, J. Shendure, J. Kitzman, M. F. Hammer, M. V. Shunkov, A. P. Derevianko, N. Patterson, A. M. Andrés, E. E. Eichler, M. Slatkin, D. Reich, J. Kelso, S. Pääbo, A high-coverage genome sequence from an archaic Denisovan individual. *Science* **338**, 222–226 (2012).
13. L. Chen, A. B. Wolf, W. Fu, L. Li, J. M. Akey, Identifying and interpreting apparent Neanderthal ancestry in African individuals. *Cell* **180**, 677–687.e16 (2020).
14. J. Krause, L. Orlando, D. Serre, B. Viola, K. Prüfer, M. P. Richards, J. J. Hublin, C. Hänni, A. P. Derevianko, S. Pääbo, Neanderthals in central Asia and Siberia. *Nature* **449**, 902–904 (2007).
15. S. Sankararaman, S. Mallick, M. Dannemann, K. Prüfer, J. Kelso, S. Pääbo, N. Patterson, D. Reich, The genomic landscape of Neanderthal ancestry in present-day humans. *Nature* **507**, 354–357 (2014).
16. I. Lazaridis, D. Nadel, G. Rollefson, D. C. Merrett, N. Rohland, S. Mallick, D. Fernandes, M. Novak, B. Gamarra, K. Sirak, S. Connell, K. Stewardson, E. Harney, Q. Fu, G. Gonzalez-Forbes, E. R. Jones, S. A. Roodenberg, G. Lengyel, F. Bocquentin, B. Gasparian, J. M. Monge, M. Gregg, V. Eshed, A. S. Mizrahi, C. Meiklejohn, F. Gerritsen, L. Bejenaru, M. Blüher, A. Campbell, G. Cavalleri, D. Comas, P. Froguel, E. Gilbert, S. M. Kerr, P. Kovacs, J. Krause, D. McGettigan, M. Merrigan, D. A. Merriwether, S. O'Reilly, M. B. Richards, O. Semino, M. Shamoon-Pour, G. Stefanescu, M. Stumvoll, A. Tönjes, A. Torroni, J. F. Wilson, L. Yengo, N. A. Hovhannysyan, N. Patterson, R. Pinhasi, D. Reich, Genomic insights into the origin of farming in the ancient Near East. *Nature* **536**, 419–424 (2016).
17. B. Vernot, J. M. Akey, Complex history of admixture between modern humans and Neandertals. *Am. J. Hum. Genet.* **96**, 448–453 (2015).
18. F. A. Villanea, J. G. Schraiber, Multiple episodes of interbreeding between Neanderthal and modern humans. *Nat. Ecol. Evol.* **3**, 39–44 (2019).
19. C. S. Quilodrán, A. Tsoupas, M. Currat, The spatial signature of introgression after a biological invasion with hybridization. *Front. Ecol. Evol.* **8**, (2020).
20. G. Barbujani, R. R. Sokal, N. L. Oden, Indo-European origins: A computer-simulation test of five hypotheses. *Am. J. Phys. Anthropol.* **96**, 109–132 (1995).
21. S. Rendine, A. Piazza, L. Cavalli-Sforza, Simulation and separation by principal components of multiple demic expansions in Europe. *Am. Nat.* **128**, 681–706 (1986).
22. C. A. Edmonds, A. S. Lillie, L. L. Cavalli-Sforza, Mutations arising in the wave front of an expanding population. *Proc. Natl. Acad. Sci. U.S.A.* **101**, 975–979 (2004).
23. S. Klopstein, M. Currat, L. Excoffier, The fate of mutations surfing on the wave of a range expansion. *Mol. Biol. Evol.* **23**, 482–490 (2006).
24. S. Peischl, I. Dupanloup, L. Bosshard, L. Excoffier, Genetic surfing in human populations: From genes to genomes. *Curr. Opin. Genet. Dev.* **41**, 53–61 (2016).
25. J. M. Travis, Deleterious mutations can surf to high densities on the wave front of an expanding population. *Mol. Biol. Evol.* **24**, 2334–2343 (2007).
26. F. Austerlitz, B. JungMuller, B. Godelle, P. H. Gouyon, Evolution of coalescence times, genetic diversity and structure during colonization. *Theor. Popul. Biol.* **51**, 148–164 (1997).
27. J. Z. Li, D. M. Absher, H. Tang, A. M. Southwick, A. M. Casto, S. Ramachandran, H. M. Cann, G. S. Barsh, M. Feldman, L. L. Cavalli-Sforza, R. M. Myers, Worldwide human relationships inferred from genome-wide patterns of variation. *Science* **319**, 1100–1104 (2008).
28. V. Sousa, S. Peischl, L. Excoffier, Impact of range expansions on current human genomic diversity. *Curr. Opin. Genet. Dev.* **29**, 22–30 (2014).
29. M. Currat, M. Ruedi, R. J. Petit, L. Excoffier, The hidden side of invasions: Massive introgression by local genes. *Evolution* **62**, 1908–1920 (2008).
30. L. N. Di Santo, C. S. Quilodrán, M. Currat, Temporal variation in introgressed segments' length statistics sheds light on past admixture pulses. *bioRxiv* 2023.05.03.539203 [Preprint]. 3 May 2023. <https://doi.org/10.1101/2023.05.03.539203>.
31. M. Currat, L. Excoffier, The effect of the Neolithic expansion on European molecular diversity. *Proc. Biol. Sci.* **272**, 679–688 (2005).
32. B. Brandt, W. Haak, C. J. Adler, C. Roth, A. Szécsényi-Nagy, S. Karimnia, S. Möller-Rieker, H. Meller, R. Ganslmeier, S. Friederich, V. Dresely, N. Nicklisch, J. K. Pickrell, F. Sirocko, D. Reich, A. Cooper, K. W. Alt; The Genographic Consortium, Ancient DNA reveals key stages in the formation of Central European mitochondrial genetic diversity. *Science* **342**, 257–261 (2013).
33. M. Lipson, A. Szécsényi-Nagy, S. Mallick, A. Pósa, B. Stégmár, V. Keerl, N. Rohland, K. Stewardson, M. Ferry, M. Michel, J. Oppenheimer, N. Broomandkoshbacht, E. Harney, S. Nordenfelt, B. Llamas, B. G. Mende, K. Köhler, K. Oross, M. Bondár, T. Marton, A. Oszás, J. Jakucs, T. Paluch, F. Horváth, P. Csengeri, J. Koós, K. Sebők, A. Anders, P. Raczy,

- J. Regenye, J. P. Barna, S. Fábíán, G. Serlegi, Z. Toldi, E. Gyöngyvér Nagy, J. Dani, E. Molnár, G. Pálfi, L. Márk, B. Melegh, Z. Bánfai, L. Domboróczki, J. Fernández-Eraso, J. A. Mújika-Alustiza, C. A. Fernández, J. J. Echevarria, R. Bollongino, J. Orschiedt, K. Schierhold, H. Meller, A. Cooper, J. Burger, E. Bánffy, K. W. Alt, C. Lalueza-Fox, W. Haak, D. Reich, Parallel palaeogenomic transects reveal complex genetic history of early European farmers. *Nature* **551**, 368–372 (2017).
34. N. M. Silva, J. Rio, S. Kreutzer, C. Papageorgopoulou, M. Currat, Bayesian estimation of partial population continuity using ancient DNA and spatially explicit simulations. *Evol. Appl.* **11**, 1642–1655 (2018).
35. Z. Hofmanova, S. Kreutzer, G. Hellenthal, C. Sell, Y. Diekmann, D. Diez-Del-Molino, L. van Dorp, S. Lopez, A. Kousathanas, V. Link, K. Kirsanow, L.M. Cassidy, R. Martiniano, M. Strobel, A. Scheu, K. Kotsakis, P. Halstead, S. Triantaphyllou, N. Kyparissi-Apostolika, D. Urem-Kotsou, C. Ziota, F. Adaktylou, S. Gopalan, D.M. Bobo, L. Winkelbach, J. Blocher, M. Unterlander, C. Leuenberger, C. Cilingiroglu, B. Horejs, F. Gerritsen, S.J. Shennan, D.G. Bradley, M. Currat, K.R. Veeramah, D. Wegmann, M.G. Thomas, C. Papageorgopoulou, J. Burger, Early farmers from across Europe directly descended from Neolithic Aegeans. *Proc. Natl. Acad. Sci. U.S.A.* **113**, 6886–6891 (2016).
36. M. E. Allentoft, M. Sikora, K. G. Sjögren, S. Rasmussen, M. Rasmussen, J. Stenderup, P. B. Damgaard, H. Schroeder, T. Ahlström, L. Vinner, A. S. Malaspinas, A. Margaryan, T. Higham, D. Chivall, N. Lynnerup, L. Harvig, J. Baron, P. D. Casa, P. Dąbrowski, P. R. Duffy, A. V. Ebel, A. Epimakhov, K. Frei, M. Furmanek, T. Gralak, A. Gromov, S. Gronkiewicz, G. Grupe, T. Hajdu, R. Jarysz, V. Khartanovich, A. Khokhlov, V. Kiss, J. Kolář, A. Kriiska, I. Lasak, C. Longhi, G. McGlynn, A. Merkevicius, I. Merkyte, M. Metspalu, R. Mkrtychyan, V. Moiseyev, L. Paja, G. Pálfi, D. Pokutta, Ł. Pospieszny, T. D. Price, L. Saag, M. Sablin, N. Shishlina, V. Smrčka, V. I. Soenov, V. Szeverényi, G. Tóth, S. V. Trifanova, L. Varul, M. Vicze, L. Yepiskoposyan, V. Zhitenev, L. Orlando, T. Sicheritz-Pontén, S. Brunak, R. Nielsen, K. Kristiansen, E. Willerslev, Population genomics of Bronze Age Eurasia. *Nature* **522**, 167–172 (2015).
37. W. Haak, I. Lazaridis, N. Patterson, N. Rohland, S. Mallick, B. Llamas, G. Brandt, S. Nordenfelt, E. Harney, K. Stewardson, Q. Fu, A. Mittnik, E. Bánffy, C. Economou, M. Francken, S. Friederich, R. G. Pena, F. Hallgren, V. Khartanovich, A. Khokhlov, M. Kunst, P. Kuznetsov, H. Meller, O. Mochalov, V. Moiseyev, N. Nicklisch, S. L. Pichler, R. Risch, M. A. R. Guerra, C. Roth, A. Szécsényi-Nagy, J. Wahl, M. Meyer, J. Krause, D. Brown, D. Anthony, A. Cooper, K. W. Alt, D. Reich, Massive migration from the steppe was a source for Indo-European languages in Europe. *Nature* **522**, 207–211 (2015).
38. J. Rio, C. S. Quilodran, M. Currat, Spatially explicit paleogenomic simulations support cohabitation with limited admixture between Bronze Age Central European populations. *Commun. Biol.* **4**, 1163 (2021).
39. L. Chikhi, R. A. Nichols, G. Barbuji, M. A. Beaumont, Y genetic data support the Neolithic diffusion model. *Proc. Natl. Acad. Sci. U.S.A.* **99**, 11008–11013 (2002).
40. Allen Ancient DNA Resource Version 50 (2022); <https://reich.hms.harvard.edu/allen-ancient-dna-resource-aadr-downloadable-genotypes-present-day-and-ancient-dna-data>.
41. K. P. Burnham, D. R. Anderson, *A Practical Information-Theoretic Approach. Model Selection and Multimodel Inference* (Springer, ed. 2, 2002).
42. M. Petr, S. Paabo, J. Kelso, B. Vernot, Limits of long-term selection against Neanderthal introgression. *Proc. Natl. Acad. Sci. U.S.A.* **116**, 1639–1644 (2019).
43. R. Nielsen, J. M. Akey, M. Jakobsson, J. K. Pritchard, S. Tishkoff, E. Willerslev, Tracing the peopling of the world through genomics. *Nature* **541**, 302–310 (2017).
44. I. Juric, S. Aeschbacher, G. Coop, The strength of selection against Neanderthal introgression. *PLOS Genet.* **12**, e1006340 (2016).
45. M. Arenas, O. Francois, M. Currat, N. Ray, L. Excoffier, Influence of admixture and paleolithic range contractions on current European diversity gradients. *Mol. Biol. Evol.* **30**, 57–61 (2013).
46. M. Arenas, N. Ray, M. Currat, L. Excoffier, Consequences of range contractions and range shifts on molecular diversity. *Mol. Biol. Evol.* **29**, 207–218 (2012).
47. N. M. Silva, S. Kreutzer, A. Souleles, S. Triantaphyllou, K. Kotsakis, D. Urem-Kotsou, P. Halstead, N. Efstratiou, S. Kotsos, G. Karamitrou-Mentessidi, F. Adaktylou, A. Chondroyianni-Metoki, M. Pappa, C. Ziota, A. Sampson, A. Papathanasiou, K. Vitelli, T. Cullen, N. Kyparissi-Apostolika, A. Z. Lanz, J. Peters, J. Rio, D. Wegmann, J. Burger, M. Currat, C. Papageorgopoulou, Ancient mitochondrial diversity reveals population homogeneity in Neolithic Greece and identifies population dynamics along the Danubian expansion axis. *Sci. Rep.* **12**, 13474 (2022).
48. D. Q. Fuller, G. Willcox, R. G. Allaby, Cultivation and domestication had multiple origins: Arguments against the core area hypothesis for the origins of agriculture in the Near East. *World Archaeol.* **43**, 628–652 (2011).
49. R. L. Bettinger, L. Barton, C. Morgan, The origins of food production in north China: A different kind of agricultural revolution. *Evol. Anthropol.* **19**, 9–21 (2010).
50. S. Riehl, M. Zeidi, N. J. Conard, Emergence of agriculture in the foothills of the Zagros Mountains of Iran. *Science* **341**, 65–67 (2013).
51. D. N. Vyas, C. J. Mulligan, Analyses of Neanderthal introgression suggest that Levantine and southern Arabian populations have a shared population history. *Am. J. Phys. Anthropol.* **169**, 227–239 (2019).
52. J. C. Ferreira, F. Alshamali, F. Montinaro, B. Cavadas, A. Torroni, L. Pereira, A. Raveane, V. Fernandes, Projecting ancient ancestry in modern-day Arabians and Iranians: A key role of the past exposed Arabo-Persian Gulf on human migrations. *Genome Biol. Evol.* **13**, evab194 (2021).
53. M. Coll Macià, L. Skov, B. M. Peter, M. H. Schierup, Different historical generation intervals in human populations inferred from Neanderthal fragment lengths and mutation signatures. *Nat. Commun.* **12**, 5317 (2021).
54. F. L. Mendez, J. C. Watkins, M. F. Hammer, A haplotype at STAT2 Introgressed from neanderthals and serves as a candidate of positive selection in Papua New Guinea. *Am. J. Hum. Genet.* **91**, 265–274 (2012).
55. H. Quach, M. Rotival, J. Pothlichet, Y. H. E. Loh, M. Dannemann, N. Zidane, G. Laval, E. Patin, C. Harmant, M. Lopez, M. Deschamps, N. Naffakh, D. Duffy, A. Coen, G. Leroux-Roels, F. Clément, A. Boland, J. F. Deleuze, J. Kelso, M. L. Albert, L. Quintana-Murci, Genetic adaptation and Neanderthal admixture shaped the immune system of human populations. *Cell* **167**, 643 (2016).
56. E. Huerta-Sanchez, X. Jin, Z. Asan, Bianba, B.M. Peter, N. Vinckenbosch, Y. Liang, X. Yi, M.Z. He, M. Somel, P.X. Ni, B. Wang, X.H. Ou, J.B. Huasang, Z.X.P. Luosang, K. Cuo, G.Y. Li, Gao, Y. Yin, W. Wang, X.Q. Zhang, X. Xu, H.M. Yang, Y.R. Li, J. Wang, J. Wang, R. Nielsen, Altitude adaptation in Tibetans caused by introgression of Denisovan-like DNA. *Nature* **512**, 194 (2014).
57. G. Kerner, E. Patin, L. Quintana-Murci, New insights into human immunity from ancient genomics. *Curr. Opin. Immunol.* **72**, 116–125 (2021).
58. H. Zeberg, S. Paabo, The major genetic risk factor for severe COVID-19 is inherited from Neanderthals. *Nature* **587**, 610 (2020).
59. N. Nakatsuka, É. Harney, S. Mallick, M. Mah, N. Patterson, D. Reich, ContamLD: Estimation of ancient nuclear DNA contamination using breakdown of linkage disequilibrium. *Genome Biol.* **21**, 199 (2020).
60. D. Reich, K. Thangaraj, N. Patterson, A. L. Price, L. Singh, Reconstructing Indian population history. *Nature* **461**, 489–494 (2009).
61. R. Maier, P. Flegontov, O. Flegontova, U. Işildak, P. Changmai, D. Reich, On the limits of fitting complex models of population history to f-statistics. *eLife* **12**, e85492 (2023).
62. A. Zuur, E. N. Ieno, N. Walker, A. A. Saveliev, G. M. Smith, *Mixed Effects Models and Extensions in Ecology with R* (Springer Science & Business Media, 2009).
63. F. Pouyet, S. Aeschbacher, A. Thiéry, L. Excoffier, Background selection and biased gene conversion affect more than 95% of the human genome and bias demographic inferences. *eLife* **7**, e36317 (2018).
64. S. Nakagawa, P. C. D. Johnson, H. Schielzeth, The coefficient of determination R<sup>2</sup> and intra-class correlation coefficient from generalized linear mixed-effects models revisited and expanded. *J. R. Soc. Interface* **14**, 20170213 (2017).
65. R Development Core Team, *R: A Language and Environment for Statistical Computing* (R Foundation for Statistical Computing, 2021).
66. J. Pinheiro, D. Bates, S. DebRoy, D. Sarkar, R Core Team, nlme: Linear and nonlinear mixed effects models. R package version 3.1-142 (2019); <https://CRAN.R-project.org/package=nlme>.
67. R. Lenth, emmeans: Estimated marginal means, aka least-squares means. R package version 1.8.6 (2023).
68. K. Barton, Package ‘MuMIn’: Multi-model inference. R package version 1.43.15; <https://CRAN.R-project.org/package=MuMIn>.
69. R. J. Hijmans, Package ‘raster’. R package **734**, 473 (2015).
70. M. Currat, M. Arenas, C. S. Quilodrán, L. Excoffier, N. Ray, SPLATCHE3: Simulation of serial genetic data under spatially explicit evolutionary scenarios including long-distance dispersal. *Bioinformatics* **35**, 4480–4483 (2019).

**Acknowledgments:** We thank P. Gerbault, P. Cerrito, and L. Di Santo for careful reading of the manuscript. **Funding:** This project was financially supported by Swiss National Science Foundation grant no. 31003A\_182577 to M.C. and no. P5R5PB\_203169 to C.S.Q. **Author contributions:** All authors contributed to the design of the study, the interpretation of the results, and the writing of the manuscript. J.R. and A.T. formatted the data. C.S.Q., J.R., and A.T. performed the analyses. A.T. performed the simulations. C.S.Q. and J.R. drafted the manuscript. M.C. coordinated the study. **Competing interests:** The authors declare that they have no competing interests. **Data and materials availability:** All data needed to evaluate the conclusions in the paper are present in the paper and/or the Supplementary Materials. The data analyzed were previously published and retrieved from the Allen Ancient DNA Resource v50.0 (<https://reich.hms.harvard.edu/allen-ancient-dna-resource-aadr-downloadable-genotypes-present-day-and-ancient-dna-data>). Data S2 lists all the genomes used in our analysis with their

indexes in the AADR database and their original references, as well as the associated population groups.

Submitted 2 February 2023  
Accepted 11 September 2023  
Published 18 October 2023  
10.1126/sciadv.adg9817

## Past human expansions shaped the spatial pattern of Neanderthal ancestry

Claudio S. Quilodrán, Jérémy Rio, Alexandros Tsoupas, and Mathias Currat

*Sci. Adv.* **9** (42), eadg9817. DOI: 10.1126/sciadv.adg9817

### View the article online

<https://www.science.org/doi/10.1126/sciadv.adg9817>

### Permissions

<https://www.science.org/help/reprints-and-permissions>

Use of this article is subject to the [Terms of service](#)

---

*Science Advances* (ISSN 2375-2548) is published by the American Association for the Advancement of Science. 1200 New York Avenue NW, Washington, DC 20005. The title *Science Advances* is a registered trademark of AAAS.

Copyright © 2023 The Authors, some rights reserved; exclusive licensee American Association for the Advancement of Science. No claim to original U.S. Government Works. Distributed under a Creative Commons Attribution NonCommercial License 4.0 (CC BY-NC).